

Droplet-Based Microreactions With Oil Encapsulation

Chuang-Yuan Lee, Hongyu Yu, *Member, IEEE*, Wei Pang, *Member, IEEE*, and Eun Sok Kim, *Senior Member, IEEE*

Abstract—This paper reports a microreaction technology for biochemical assay using nanoliter droplets encapsulated inside oil droplets. Microreaction chambers are constructed on a glass substrate by accumulating oil droplets that are dispensed by a directional droplet ejector. Droplets of different aqueous reagents are then directionally ejected (by other directional droplet ejector adjacent to the oil droplet ejector) into the oil microchambers for parallel and combinatory analysis. Because the reagents are encapsulated in oil, the evaporation rate is reduced by several orders of magnitude, and only small amounts of reagents are required for each assay. The microchamber size and the reagent amount are digitally controlled by the number of ejected oil and reagent droplets, respectively. The ejectors for oil and reagents have been integrated on a single chip so that each assay is performed efficiently without any mechanical movement and alignment. We have carried out both physical and chemical microreactions with this method and observed a negligible difference in response from conventional macroreactions. [2007-0097]

Index Terms—Acoustic devices, microactuators.

I. INTRODUCTION

MICROFLUIDIC networks are useful for experiments that require minimal use of reagents and have been used in fields ranging from analytical chemistry to biomedicine [1]–[3]. In principle, a microfluidic system can offer high throughput at a reduced cost by densely integrating complex biochemical assays on a chip. Although the first microfluidic chips were fabricated by etching a substrate such as silicon [4] and glass [5] with conventional photolithography, more and more devices are made by molding elastomers such as silicone [6] and polydimethylsiloxane [7] with soft lithography due to their low production cost.

In most of the reported microfluidic networks, liquids travel through sealed interconnect channels, which are embedded into a solid matrix. The mass transfer of liquid mediums in

these systems is dominated by diffusion due to the small Reynolds number [8]. The liquid flow can be manipulated by a pressure difference in the conduits. However, the passive pressure-driven networks typically have a broadened velocity profile and suffer from reagents' diffusion through junctions and channels over time [9]. Another drawback is that the pressure-driven flows do not scale well with miniaturization and often require complicated off-chip plumbing [10]. Alternatively, electro-osmotic flow can be used for liquid transport with more homogeneous velocity distribution and better scalability with miniaturization due to its lack of any moving parts [11]. However, with the incorporation of the active electrical or pneumatic pumping mechanisms into the microfluidic networks, the interface complexity will also increase. Moreover, a practical issue for all these systems with complex microchannel networks is the priming problem of filling the device with fluids. In addition to the potential contamination of the samples, the initial introduction of fluids can also generate undesirable air bubbles [12].

Liquids can also be confined and guided on open surfaces without a closed conduit, and several approaches have been developed to pattern the wettable areas on a surface, including electrowetting using an array of electrodes [13], wedge wetting by patterning the surface topology [14], and chemical wettability engineering [15]. The main disadvantage of these open microfluidic systems is the inevitable contamination and drying of the liquid samples.

Another candidate for the miniaturization of microfluidic systems is inkjet technology. The inkjet printing is able to deliver droplets on demand and can be potentially applied to the nanoliter-scale assays [16]. However, like other droplet-based technologies, once the droplet has been dispensed, the fast evaporation of liquid would prevent it from further use in accurate and effective assays [17]. Therefore, the major challenge is to carry out the experiments utilizing small droplets and yet to overcome the problematic liquid evaporation as well as contamination that may happen without any closed channel networks. One prospective solution is to encapsulate the aqueous droplets with oil by taking advantage of the immiscibility between water and oil [13], [18]–[20].

Here, we present a new microfluidic platform for biochemical assays using directional acoustic ejectors without complex channel networks. Acoustic actuation is employed because the commercial inkjet print heads shoot out liquid droplets through nozzles by either thermal or piezoelectrical actuation and have difficulty to dispense oil with large viscosity. In addition, although directional ejection can be achieved for nozzle-based

Manuscript received May 2, 2007; revised August 25, 2007. This work was supported by the National Science Foundation (NSF) under Grant ECS-0310622. Subject Editor Y. Zohar.

C.-Y. Lee is with the Department of Electrical Engineering—Electrophysics, University of Southern California, Los Angeles, CA 90089 USA (e-mail: chuanyl@usc.edu).

H. Yu is with the Department of Electrical Engineering and the Department of Biomedical Engineering and Cardiovascular Medicine, University of Southern California, Los Angeles, CA 90089 USA.

W. Pang is with the Wireless Semiconductor Division, Avago Technologies, Inc., San Jose, CA 95131 USA.

E. S. Kim is with the Department of Electrical Engineering, University of Southern California, Los Angeles, CA 90089 USA.

Color versions of one or more of the figures in this paper are available online at <http://ieeexplore.ieee.org>.

Digital Object Identifier 10.1109/JMEMS.2007.911873

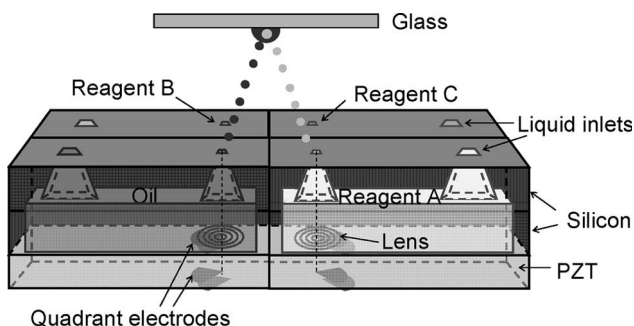


Fig. 1. Schematic diagram of a droplet-based microreaction platform based on four directional acoustic ejectors (two in the front and the other two in the back) along with four inlet ports. With a footprint of 20×10 mm, the overall chip is constructed with a stack of two $400\text{-}\mu\text{m}$ -thick micromachined silicon chambers and a $127\text{-}\mu\text{m}$ -thick PZT transducer.

ejectors, they typically require an external electric field or heater to alter the direction. In the piezoelectric method, a hydrostatic pressure is produced by the mechanical bending of a piezoelectric unimorph or diaphragm to eject the droplets out of a nozzle. In contrast, acoustic ejection is a nozzleless droplet generation method in which an acoustic beam is focused on the liquid surface to overcome the restraining force of the surface tension and to expel the droplet from an open space without any nozzle [21]. It is the high-intensity sound beam, not the mechanical bending associated with piezoelectric actuation, that acts to eject droplets. As a result, droplets of both aqueous and nonaqueous fluids (even oil droplets with a viscosity of 55 cSt) can be easily dispensed by an acoustic ejector [22]. In addition to the ability of oil dispensation, the acoustic ejector with patterned electrodes is capable of ejecting droplets in directional angles without an external electric field. Thus, the directional ejection can reduce the mechanical movements needed to perform a combinatory biochemical assay. In this new microfluidic platform, we first construct an array of oil microreaction chambers on a glass substrate by acoustically ejecting and accumulating oil droplets and then eject droplets of different aqueous reagents into the oil microchambers. With the oil encapsulation, the evaporation of the reagents can be better controlled for miniaturized assays.

II. DESIGN

The schematic diagram of the proposed microreaction platform based on directional acoustic ejectors is shown in Fig. 1. An array of four directional acoustic ejectors (integrated with four separate reservoirs and four inlet ports) is constructed on a lead zirconate titanate (PZT) substrate. The ejector mainly consists of an acoustic transducer and a lens with air-reflectors (LWAR) [23]. The PZT transducer, which is operated at the fundamental thickness-mode resonant frequency, is used to generate acoustic waves which are then focused by the LWAR to eject liquid droplets without any nozzle. LWAR is an acoustic lens patterned into annular Fresnel half-wave rings, where the odd-numbered rings are constructed with parylene and the even-numbered rings are made of air. By taking advantage of the fact that air has an acoustic impedance that is much smaller than that of any solid, LWAR provides a method to

focus the acoustic waves. Due to impedance mismatch, the acoustic waves produced by the PZT transducer can propagate into water through the parylene but are mostly reflected by the air pockets. Then, the transmitted acoustic waves arrive at the focal point in phase, constructively interfering with each other and intensifying the acoustic pressure. The ejected droplet size is primarily determined by the diameter of the focused acoustic beam at the focal plane that is related to the acoustic wavelength and the aperture of the acoustic lens [24].

For efficient droplet ejection, the focus of the acoustic energy should be constantly kept at the liquid surface. For acoustic ejectors without reservoirs, the liquid level would drop as the liquid is ejected out. Since the acoustic lens has a fixed focal length, there must be an adjustable acoustic coupling layer between the transducer and the liquid chamber so that the transducer can be dynamically moved for stable ejection [25]. The relative position between the transducer and the liquid surface can be determined by the sonar method, in which the time duration of the echo returned to the transducer from the liquid/air interface is recorded. The sonar method, together with electrical feedback, can thus ensure an efficient droplet ejection. In the new reservoir design, the integrated reservoirs are directly connected to the ejection chambers, and liquid can be continuously delivered to replenish the ejection chambers, where the liquid level is maintained at the top surface of the silicon chamber without any electrical feedback. Since the liquid medium is in direct contact with the lens made of parylene (that is biocompatible), the acoustic ejector is suitable for various biochemical applications.

In general, several reagents are needed for one biochemical assay, and the 2-D array of 2×2 ejectors having “pie-shaped” sector electrodes is integrated on a single chip for efficient analysis. As both top and bottom electrodes are patterned into the “pie-shaped” sector electrodes, droplets are ejected in a direction oblique to the liquid surface. Consequently, the ejector array does not have to be mechanically aligned to spot one point (on a glass or any other assay substrate) with different liquids. One of the ejectors is used to eject oil droplets, and the other three ejectors are for different targeted reagents. As each assay is performed without any mechanical movement and alignment, the control circuitry and automation is considerably reduced.

The microreactions using nanoliter droplets with oil encapsulation are performed according to the following sequence. First, we directionally eject and collect oil droplets on the glass substrate to form oil microreaction chambers, where reaction will take place inside. Because the acoustic ejector can eject one liquid droplet per one electrical pulse, the microchamber size (V_{MC}) can be digitally controlled by the number of ejected oil droplets (N) (i.e., $V_{MC} = N \times V_D$, where V_D is the volume of one ejected droplet). After the oil microchambers are constructed, droplets of reagents are then directionally ejected into the microchambers for reaction. A combinatory assay not only entails utilization of numerous reagents but also involves different trials using various dosages (or concentration) of individual reagent. The dispensation of reagents can be carried out either sequentially or concurrently, and the reagent dosage is also digitally controllable by the number of ejected reagent droplets.

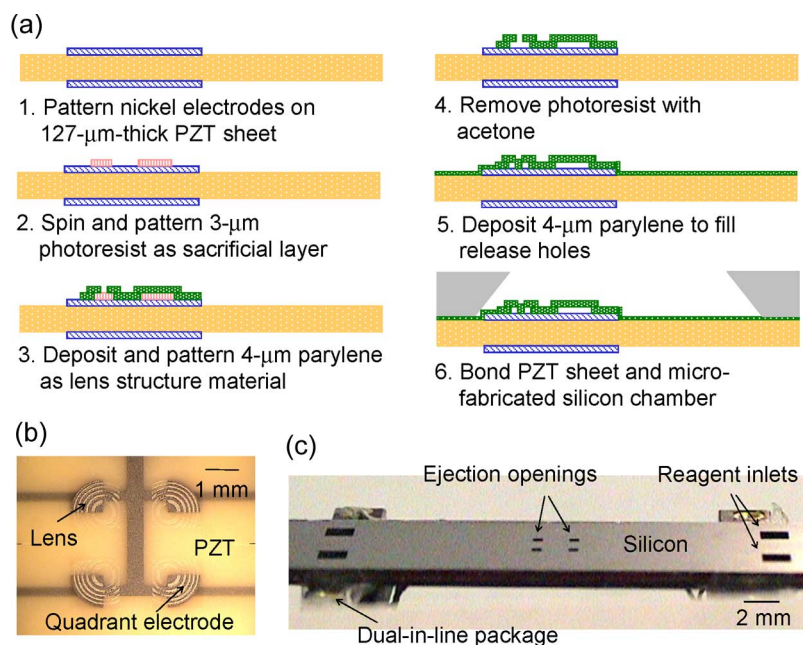


Fig. 2. Fabrication of the microreaction platform based on four directional acoustic ejectors. (a) Device fabrication steps. (b) Photo of the fabricated PZT ejector array. (c) Photo of the finished device mounted on a DIP.

Since only one reagent is to be run through a single ejector, which is integrated with its own microchannel and reservoir, the individual ejectors dispense discrete droplets without cross contamination. In addition, because the microreaction is carried out inside the oil, the contamination and evaporation of the reagents are greatly reduced, and thus, the assay volume is miniaturized. With each microchamber representing one individual assay, this microreaction platform allows complex but economical high-throughput combinatory analysis easily through a computer program.

III. FABRICATION AND TESTING

The PZT ejector array and silicon reservoirs were fabricated, as described in the following, according to the processing steps shown in Fig. 2(a). The acoustic ejector was built on a 127- μm -thick PZT sheet (PSI-5A4E, Piezo Systems). On both sides of the PZT sheet, nickel electrodes were first patterned into quadrant sectors. Next, a 3- μm -thick photoresist was spun and patterned as the sacrificial layer. After depositing and patterning a 3- μm -thick parylene as the lens material, we removed the photoresist with acetone. Another 4- μm -thick parylene was then deposited to fill the release holes.

The microfluidic components (embedded microchannels, ejection chambers, and reservoirs) were microfabricated with two silicon wafers. Both sides of the silicon wafers were first deposited with 0.8- μm -thick Si_xN_y by low-pressure chemical vapor deposition. The front-side Si_xN_y was then patterned, followed by anisotropic etching of bulk silicon in KOH. After etching silicon for the microfluidic components, the Si_xN_y was removed, and two silicon wafers were bonded together with epoxy. Finally, the PZT sheet was adhesively bonded to the silicon wafers. The photo of the fabricated PZT ejector array is shown in Fig. 2(b), and the photo of the finished device

mounted on a dual-in-line package (DIP) is shown in Fig. 2(c), where we denote the inlet ports for liquid refilling and the openings ($500 \times 500 \mu\text{m}$) for ejections.

For the device testing, an 18-MHz sinusoidal pulse was applied to the ejectors to eject liquid droplets in a setup shown in Fig. 3. First, the sinusoidal signal was modulated with radio-frequency (RF) pulses through a high-speed switch. The pulse repetition frequency (PRF) used was ranging from 1 Hz to 10 kHz, and the pulsewidth was from 7 to 100 μs . The pulsed signal was then amplified with an RF power amplifier (A041, LCF Enterprises) and split into four signals through a power splitter and an RF switch array before being applied to each of the four ejectors. Each ejector was individually actuated by a computer program. A glass substrate was placed above the device to collect the ejected droplets of oil and reagents. The inset in the figure shows the glass substrate and the testing device electrically connected to four SMA connectors on a mounting stage. A charge-coupled device camera (SONY SSC-DC54A) with a microscope was placed horizontally to record the ejection process as we stroboscopically blinked a light-emitting diode (LED). Synchronization of the flash illumination with the sinusoidal pulse input was achieved by turning on the LED with another pulse source triggered by the pulse generator that pulsed the sinusoidal signal. By varying the delay time between the illumination of LED and the RF signal applied to the transducer, we observed the ejection process at any moment.

IV. RESULTS AND DISCUSSION

A. Construction of Oil Microreaction Chambers

The first step for the droplet-based microreactions with oil encapsulation is to construct the oil microchambers. We

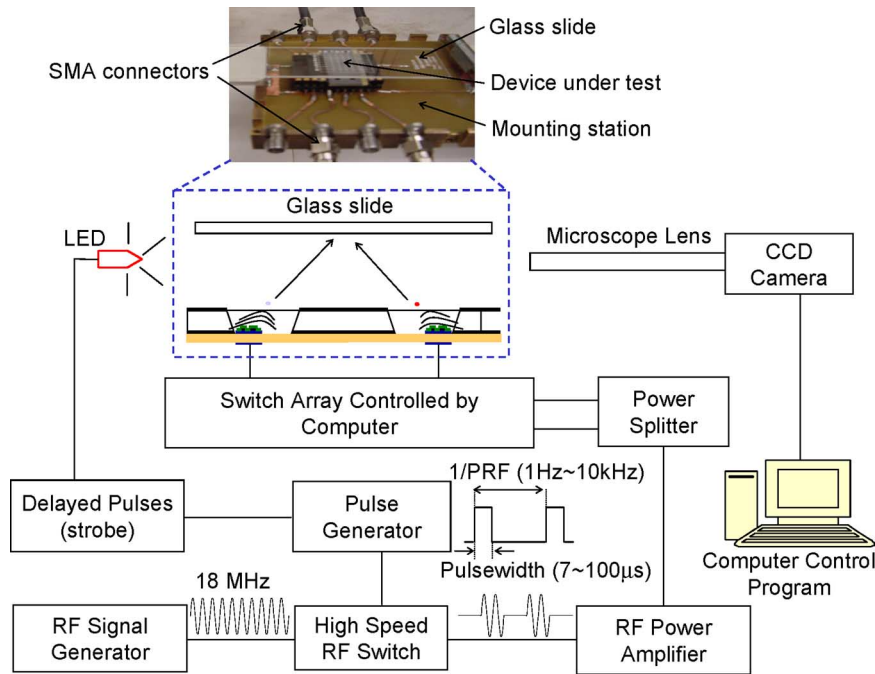


Fig. 3. Experimental setup for microreactions on a glass slide using directional acoustic ejectors of which the ejection sequence was controlled through a computer program. Device was mounted on a mounting station and connected through SMA connectors.

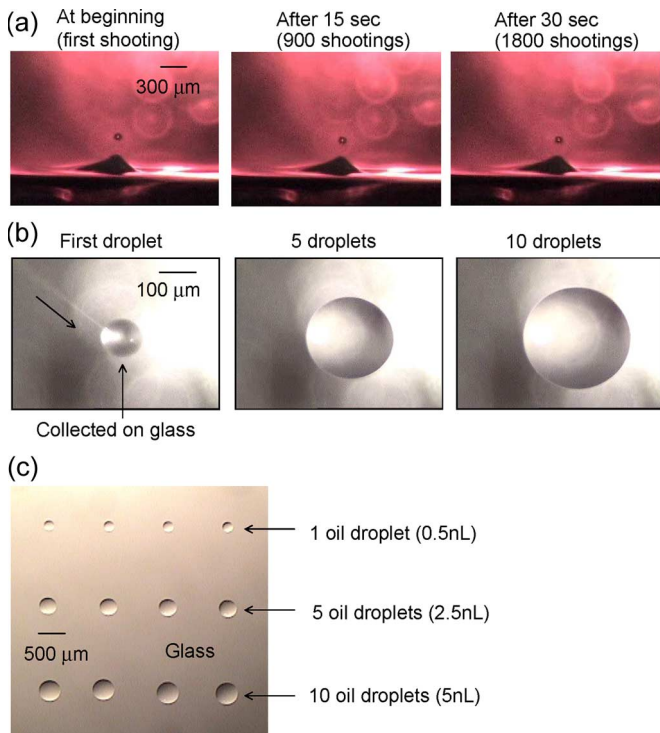


Fig. 4. Construction of oil microreaction chambers. (a) Stable and continuous directional ejections of oil droplets without any frequency tuning. (b) Successive oil droplets ejected onto the same position on glass and accumulated into oil microchamber. (c) Array of oil microchambers constructed on glass substrate.

first examined the ejection of oil droplets from the side-view micrographs. The oil used was Inland-19 Ultra with a viscosity of 55 cSt. Fig. 4(a) shows the continuous ejections driven with ± 60 -V_{peak-to-peak} pulses of 18-MHz sinusoidal signals

without any fine frequency tuning. The pulsewidth and the PRF were 100 μ s and 60 Hz, respectively. The ejection was one oil droplet per pulse and free of satellite droplets. The frame taken at the beginning of the ejections is almost identical to the one after 30 s of ejections (1800 droplet shootings), exhibiting the uniformity of droplet sizes and the stability of the ejection process. For the same ejector driven with the same electrical condition, there is no obvious variation in the droplet size. For a set of eight ejectors, the ejected oil droplets have a diameter ranging from 95 to 106 μ m, possibly caused by the resonance frequency variations from the PZT substrate and the liquid level variations due to the difference in epoxy layer thickness. The mean diameter is 101 μ m with a standard deviation of 2.5 μ m for the eight ejectors.

To construct the oil microreaction chambers, we next tested the oil ejection with a glass substrate placed 1 cm above the ejector and examined the ejection process from the top view. In order to clearly see the oil droplets accumulate through time, a low PRF was intentionally used for the testing. The oil droplets were directionally ejected and collected as the microchambers on the glass. The droplet position was so consistent that sequential droplets hit at the same spot and that the oil microchamber grew through time, demonstrating the precise directionality for every droplet ejection [Fig. 4(b)].

After the ejection characterization, oil droplets were then systematically ejected to form microreaction chambers on a glass substrate. Because an oil microchamber can hold a limited amount of reagents before its breakdown, a larger microchamber is generally needed for a greater amount of reagents. With this drop-on-demand capability, the microchamber size was digitally controlled by the number of ejected oil droplets, and an array of oil microchambers with different sizes was formed [Fig. 4(c)].

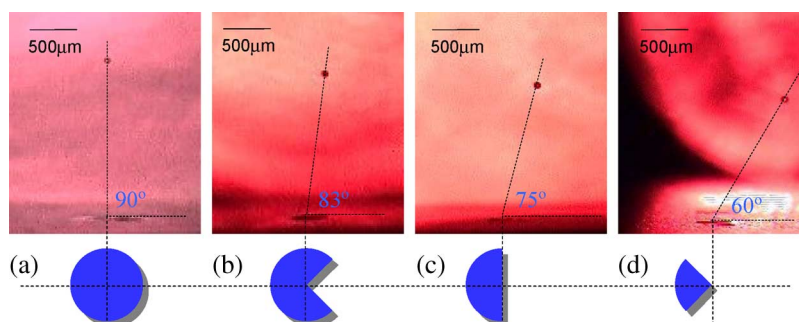


Fig. 5. Variation in directional ejection angles by different sector electrode patterns.

TABLE I
SIMULATION OF PARTICLE DISPLACEMENTS ON THE LIQUID SURFACE AND EXPERIMENTAL DIRECTIONAL EJECTION ANGLES FOR DIFFERENT ELECTRODE PATTERNS

	Apex angle of sectored electrode (deg)	360	270	180	90
					
Simulation	Normalized particle displacement	8.1	6.4	4.4	2.0
	Ratio of lateral to vertical particle displacement	0	0.16	0.37	0.59
Experiment	Tilting angle from vertical direction (deg)	0	7	15	30

B. Directionality Manipulation by Electrode Design and Electrical Pulswidth

The ejection directionality can be altered through an electrode design before the ejector fabrication and can also be dynamically controlled after the ejector is fabricated. Rather than a “circular” electrode, a “pie-shaped” electrode that we call “sector” shape is used for directional ejections. Fig. 5 shows the water ejections by ejectors with different sector electrode patterns. Driven with RF pulses (± 60 V_{peak-to-peak} with 60-Hz PRF) of 18-MHz sinusoidal signals, it is demonstrated that the ejection becomes more tilting as the sector angle gets smaller. This trend is in agreement with the simulation results which show that as the sector angle decreases, the vertical particle displacement at the liquid surface becomes less intensified, while the relative lateral displacement becomes larger (Table I). For the same ejector driven with the same electrical condition, there is no obvious variation in ejection directionality. For a set of eight ejectors, the directional angle varies within $\pm 3^\circ$. This is possibly due to the fact that the PZT ejector was manually bonded to the silicon chamber and that the misalignment of the ejector to the ejection opening would result in a different boundary condition for the ejection. In addition, the relatively large undercut of the nickel electrodes on the PZT may also cause the electrode-pattern variation among the devices and influence the directional angle.

For liquids with various surface tensions and densities, the ejection direction could be different with the same electrode pattern. We can adjust the directionality by varying the electrical pulswidth. Although the pulswidth effect on acoustic ejection remains unclear for lack of theory [24], in the case of directional ejection, we found that the directionality is a function of pulswidth and that a larger pulswidth would result in a less oblique ejection angle. Fig. 6 shows the direction

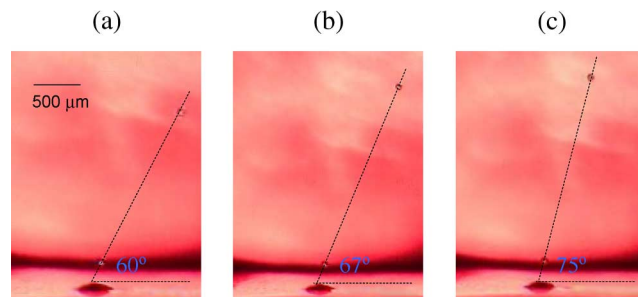


Fig. 6. Variation in directional ejection angles by different pulswidth settings for an ejector with 90° sectored electrodes. (a) Pulsewidth = $7 \mu\text{s}$. (b) Pulsewidth = $12 \mu\text{s}$. (c) Pulsewidth = $15 \mu\text{s}$.

tunability (from 60° to 75°) of the same ejector (with a quadrant sector) with different pulswidth values (± 60 V_{peak-to-peak} with 1-kHz PRF).

Since the ejection direction depends on electrode patterns, another way to dynamically manipulate the ejection angle is to divide the circular electrode of one ejector into various equal sectors. By dividing the electrode into M sectors, the ejection can be controlled into $2^M - 1$ different angles through combinatory activations of any $1, 2, 3, \dots, M$ sectors.

C. Dispensation of Reagent Droplets Into Oil Microchambers

After the construction of oil microchambers, the next step for microreaction is to eject the reagent droplets into the oil microchambers. For easy visualization of the dispensation process, the diluted red ink was first used as the liquid medium. We formed the microchamber by accumulating 20 oil droplets on the glass and then directionally ejected the red ink droplets ($80 \mu\text{m}$ in diameter) into the oil by another ejector with ± 60 -V_{peak-to-peak} pulses of 10 - μs pulswidth [Fig. 7(a)].

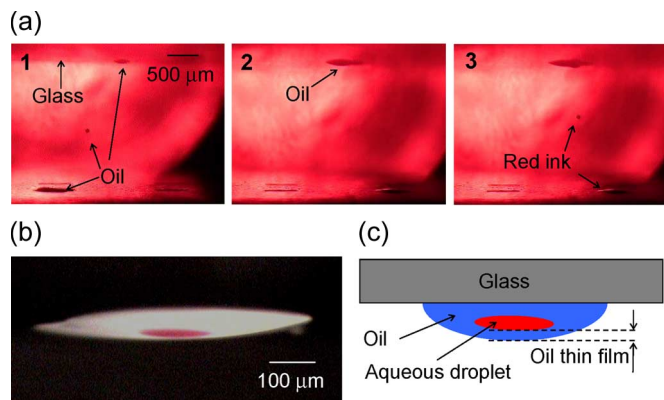


Fig. 7. Dispensation of red ink droplet into the oil microreaction chamber. (a) Sequential steps to form oil microreaction chamber and to dispense red ink droplet: (1) Oil droplets ejected by directional ejector and collected on glass; (2) microreaction chamber constructed with 20 oil droplets; and (3) ejection of red ink droplets. (b) Photo showing red ink droplet encapsulated inside the oil. (c) Schematic showing relative position of encapsulated aqueous droplet inside the oil.



Fig. 8. Detailed sequence of encapsulation process. Water was used as the liquid medium. One water droplet was ejected onto oil to create a water crater, which was then sealed radially from the outside by a thin film of oil.

The droplet landing position could easily be controlled within 80 μm from ejection to ejection. Since the first two successive droplets always overlap each other, the landing-position accuracy is conservatively estimated to be within one droplet size. The ink droplet penetrated through the oil–air interface and was wrapped by a thin film of oil [Fig. 7(b)]. The droplet stopped as its kinetic energy was balanced by the viscous loss from the drag force that resisted the motion. The ink droplet was placed very close to the oil–air interface and isolated from air ambient by a thin oil film, as shown in Fig. 7(c). By flipping over the glass substrate and yet attaining the same relative position of the encapsulated aqueous droplet inside the oil, we confirmed that the aqueous droplet's proximity to the oil–air interface (rather than the oil–glass interface) was not caused by the gravity effect.

Fig. 8 shows the detailed encapsulation sequence from another point of view. One water droplet was ejected into the oil microchamber. As the water droplet first impacted the oil, it created a crater. The water crater was then sealed by a thin film of oil radially from the outside and completely encapsulated inside the oil in less than 0.7 s.

In addition, we have proposed and performed another scheme for the droplet-based microreactions with oil encapsulation. Fig. 9 shows the schematic representation of the alternative scheme. Instead of forming the oil microchamber first by ejecting oil droplets onto the glass substrate, we dispensed the reagent droplets directly through an oil film for oil encapsulation. We formed the oil film by surface tension. A 160-μm-thick copper wire was shaped into a hydrophilic metal frame, around which the oil film was suspended. The aqueous reagent

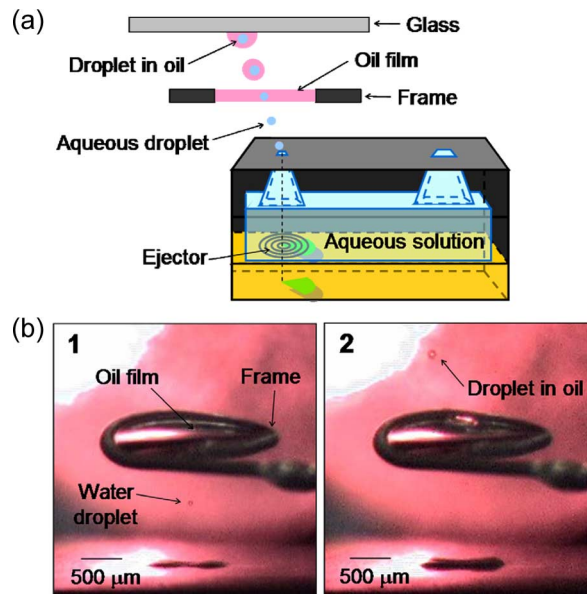


Fig. 9. Alternative scheme for droplet-based microreactions with oil encapsulation. (a) Schematic representation of the alternative scheme. Aqueous droplets were dispensed to penetrate through an oil film for oil encapsulation. (b) Experimental results showing a liquid droplet before and after it passed through the oil film: (1) Water droplet ejected toward the oil film constructed by a metal frame; and (2) water droplet encapsulated in oil after penetration through the oil film.

droplets were then ejected to penetrate through the oil film and then wrapped with oil after penetration. However, there exist several drawbacks with this method. First, since some portion of the oil is taken away with the flying reagent droplet for oil encapsulation, a more complicated microfluidic system will be needed to dynamically supply and reconstruct the oil film upon oil consumption. Second, during the penetration process, some reagent residues are undesirably left in the oil, resulting in cross-contamination issues for subsequent reactions. Third, since many reagents are typically required for one assay, reagent droplets have to first coalesce in air and then go through oil film for encapsulation. It becomes extremely challenging particularly when many droplets are needed for digital control of the reagent amount. Thus, although this alternative method can also be employed for oil encapsulation, it will not be too practical until the mentioned issues are resolved.

D. Characterization of Water Evaporation Rate

Evaporation rates of droplets with and without oil encapsulation were characterized. When one water droplet was ejected into the microchamber formed by ten oil droplets, the evaporation rate with the oil encapsulation was so slow that it took more than 10 h for the droplet of only around 0.27 nL to evaporate [Fig. 10(a)]. In a control test, a water droplet of the same volume was observed to spread and dry out within 3 s after being ejected onto a glass surface without any oil encapsulation. This kind of fast evaporation is the main challenge in carrying out any biochemical experiment with a small reagent amount. Thus, with the oil encapsulation, miniaturized assays using reagent volumes of only nanoliters are achievable.

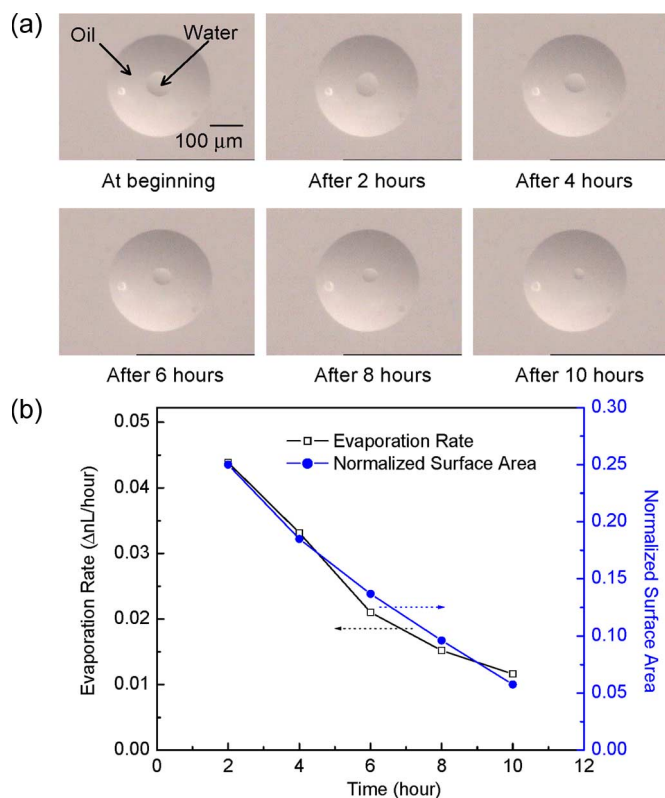


Fig. 10. Characterization of water evaporation rate. (a) Photos showing slow evaporation of one water droplet (~ 0.27 nL) inside the ten-oil-droplet microchamber. It took more than 10 h for the water droplet to dry out. (b) Measured decrease in evaporation rate as a function of time. Also plotted is the surface area, over which diffusion is taking place, as a function of time.

Although it was difficult to measure the thickness of the oil film between the water and air either from the side- (Fig. 7) or top-view micrograph (Fig. 8), it can be estimated by calculating the water evaporation rate. According to the Fick's law of diffusion [26], the water encapsulated in oil evaporates at a rate given by

$$\frac{\partial Q}{\partial t} = \frac{AD(P_{\text{sat}} - P_a)}{lRT} \quad (1)$$

where A is the surface area over which diffusion is taking place, D is the diffusion coefficient of water in oil, P_{sat} is the saturation water vapor pressure in the air, P_a is the actual water vapor pressure in the air, l is the oil film thickness, R is the universal gas constant, and T is the air temperature. The measured decrease in evaporation rate as a function of time is shown in Fig. 10(b). The evaporation rate is observed to be directly proportional to the droplet surface area, indicating that the oil thin-film thickness remains about the same throughout the 10 h. With the experimental evaporation results, the oil film was calculated to be around $0.5 \mu\text{m}$. Although the oil film was thin, it has been proven to be very efficient in reducing the evaporation rate.

E. Physical Mixing Reaction

A series of microreaction applications has been performed with the new method. First, we conducted a physical mixing

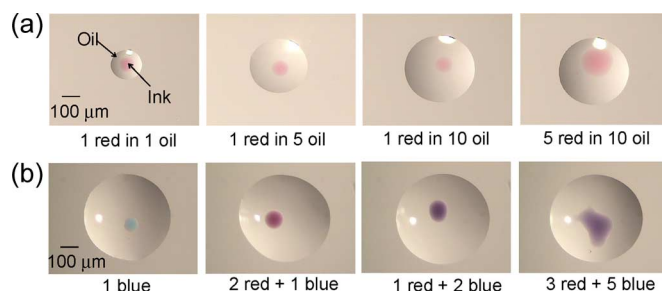


Fig. 11. Physical mixing microreaction using nanoliter droplets with oil encapsulation. (a) Micrographs showing red ink droplets ejected and encapsulated inside oil microchambers with different sizes. (b) Micrographs showing various combinations of red and blue ink droplets encapsulated and mixed inside the oil microchamber.

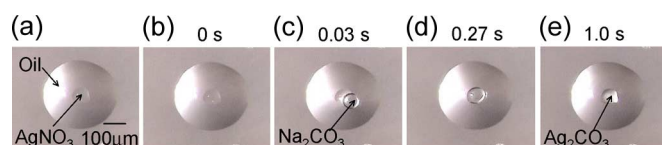


Fig. 12. Chemical precipitation microreaction using nanoliter droplets with oil encapsulation. (a) One droplet of 0.1-M silver nitrate solution ejected and encapsulated inside the oil. (b) No observable evaporation after 1 h. (c) Dispensation of one droplet of 0.1-M sodium carbonate solution into oil. (d) Microreaction of silver nitrate and sodium carbonate with oil encapsulation. (e) Formation of silver carbonate precipitate in 1 s.

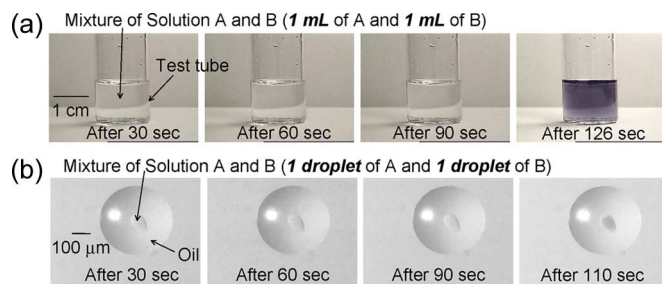


Fig. 13. Long-term iodine clock reaction. (a) Macroreaction: Pipetting 1 mL of solution A and 1 mL of solution B into test tube for reaction. Blue color appeared after 126 s [mixture of solutions A and B (1 mL of A and 1 mL of B)]. (b) Microreaction: Ejecting one droplet (0.3 nL) of solution A and one droplet (0.3 nL) of solution B into oil microchamber for reaction. Blue color appeared after 110 s [mixture of solutions A and B (1 droplet of A and 1 droplet of B)].

experiment. We formed the microchambers by ejecting and accumulating oil droplets on the glass slide and then dispensed the diluted ink droplets into the oil. It has been demonstrated that the ink droplets can be dispensed and encapsulated into the oil microchambers of different sizes [Fig. 11(a)]. In addition, various combinations of red and blue ink droplets were ejected and mixed by diffusion inside the microchamber and showed an expected color mixing even with the assay volume in the range of only nanoliters. Fig. 11(b) shows the mixing results 5 s after ink droplets were ejected and encapsulated inside the oil microchamber.

F. Chemical Precipitation Reaction

Not only can the physical reaction be carried out inside the oil but also the chemical reaction can be completed with this method. For visual demonstration, we have used the microreaction platform to perform the precipitation reaction. As silver

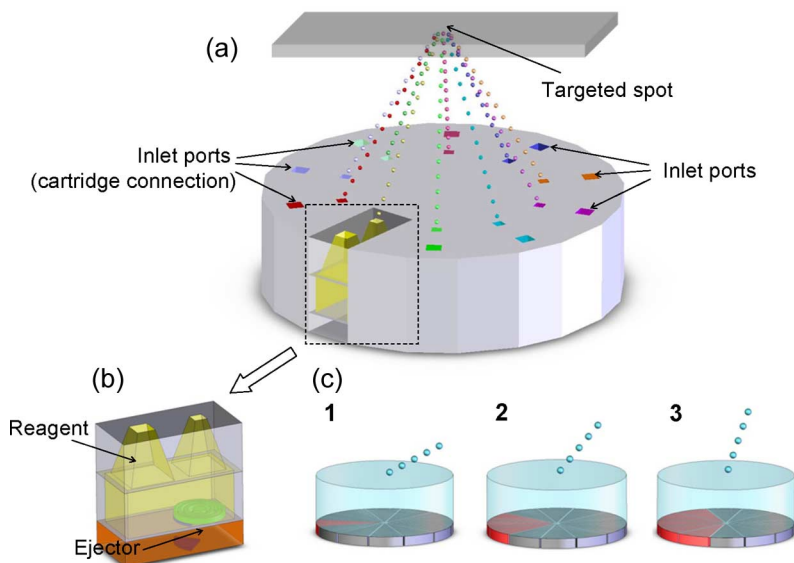
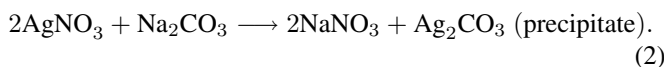


Fig. 14. Schematic representation of an exemplary array of ten ejectors for droplet-based microreactions. (a) Diagram showing ten ejectors (along with ten peripheral inlet ports) targeting the same spot in the center with ten different liquids. (b) Detailed perspective drawing of a composed unit of the array. (c) Demonstration of dynamic control of ejection angle through combinatory actuation of any sector electrode: (1) Actuation of one sector for most oblique ejection angle; (2) actuation of three sectors for less oblique ejection angle; and (3) actuation of five sectors for least oblique ejection angle (electrodes of one ejector are divided into 12 equal sectors in this example).

nitrate reacts with sodium carbonate, they exchange partners to form silver carbonate, which cannot be dissolved in water [27]

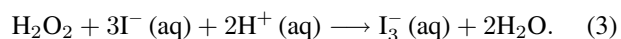


We prepared two colorless solutions—0.1-M silver nitrate and 0.1-M sodium carbonate. After we ejected and collected ten oil droplets to form the microreaction chamber, one droplet (~ 0.3 nL) of the silver nitrate solution was then dispensed into the oil [Fig. 12(a)]. After intentionally waiting 1 h to confirm negligible water evaporation [Fig. 12(b)], we then ejected one droplet (~ 0.3 nL) of the sodium carbonate solution into the microchamber for reaction [Fig. 12(c) and (d)]. The silver carbonate precipitate was attained in about 1 s, consuming only one droplet of silver nitrate and one droplet of sodium carbonate [Fig. 12(e)].

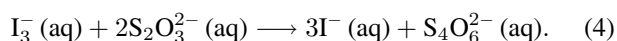
The physical mixing and chemical precipitation reactions are the assays that happen instantaneously or in seconds. The evaporation rate with oil encapsulation is so slow that this microreaction platform can even be applied for the experiments that require longer time to be completed, as shown in the next paragraph.

G. Long-Term Iodine Clock Reaction

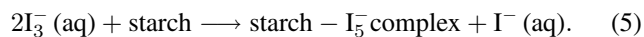
We have further demonstrated the use of the method for long-time reactions by conducting the iodine clock reaction [28], in which two colorless solutions are mixed. At first, there is no visible reaction, but the mixed solution suddenly turns blue after some time delay. There are three reactions occurring in the mixed solution. In the first reaction, iodide ions are oxidized by hydrogen peroxide to form triiodide ions in an acid solution



In the second reaction, the triiodide ions are reconverted back to iodide ions by thiosulfate



Since the second reaction is much faster than the first reaction, the triiodide ions are consumed right after they are formed, preventing any observable response in the following third reaction. After all the thiosulfate ions are used up, the triiodide ions react with starch and produce blue starch-pentaidode complex, at which point blue color appears



We prepared two colorless solutions: solution A (0.3% w/v starch, 0.003-M sodium thiosulfate, and 1.6% w/v potassium iodide in the acetate buffer, pH 4.5) and solution B (0.1% hydrogen peroxide). For demonstration, both the microreaction using the new platform and a conventional macroreaction using test tubes and pipettes have been carried out.

For the macroreaction, 1 mL of solution A and 1 mL of solution B were separately pipetted into the test tube for reaction. There was no visible color change in the beginning [Fig. 13(a)], and the blue color was observed after 126 s.

For the microreaction, one droplet (0.3 nL) of solution A and one droplet (0.3 nL) of solution B were ejected into the oil microchamber for reaction. Compared with the macroreaction, this was 3 million times reduction in the reagent volume. Similarly, there was no observable response in the beginning [Fig. 13(b)]. The blue color appeared after 110 s, which is very close to the response time of the macroreaction with 13% deviation. The difference was possibly caused by droplet evaporation during its flight in air that would have made the solutions for the microreaction be a little more concentrated than those for the macroreaction. To minimize the deviation,

the distance between the ejector and the assay substrate should be kept as close as possible to reduce the droplet evaporation. Since the distance is governed by the ejector geometry and also by the directional angle, one can use thinner piezoelectric layers to reduce the ejector size and/or increase the ejection angle further through electrode design.

For combinatory analysis involving more kinds of reagents, an array of more ejectors can easily be designed and integrated on a single chip. Fig. 14 shows an exemplary array of ten ejectors targeting the same spot in the center. Connections to cartridges for refill can be achieved peripherally through inlet ports for individual ejector. In addition, by dividing the electrode of one ejector into equal sectors and combinatorially activating any combination of the sectors [Fig. 14(c)], the ejection angle can be dynamically manipulated to compensate the direction variation due to utilization of reagents with different viscosities and densities.

V. CONCLUSION

A new biochemical microreaction platform based on directional acoustic ejectors has been demonstrated. Nanoliter droplets of reagents are utilized for miniaturized assays with oil encapsulation. This microreaction technology offers the following advantages for biochemical analysis. First, the acoustic ejectors are capable of ejecting both aqueous and nonaqueous fluids. Thus, the ejectors for oil and reagents can be integrated on a single chip to target one spot on the assay substrate so that each assay is performed efficiently without any mechanical movement and alignment. Second, by dispensing the oil and reagents droplet by droplet, we can digitally control the oil microchamber size and the reagent amount easily through a computer program. Third, with the oil encapsulation, the reagent evaporation rate is greatly reduced, and the required reagent amount can be miniaturized. The method has the potential to systematically perform economical high-throughput analysis and is ideal for parallel and combinatory microreactions on a chip.

REFERENCES

- [1] A. Khademhosseini, R. Langer, J. Borenstein, and J. P. Vacanti, "Microscale technologies for tissue engineering and biology," *Proc. Nat. Acad. Sci. U.S.A.*, vol. 103, no. 8, pp. 2480–2487, Feb. 2006.
- [2] M. Joanicot and A. Ajdari, "Droplet control for microfluidics," *Science*, vol. 309, no. 5736, pp. 887–888, 2005.
- [3] J. Sager, M. Young, and D. Stefanovic, "Characterization of transverse channel concentration profiles obtainable with a class of microfluidic networks," *Langmuir*, vol. 22, no. 9, pp. 4452–4455, 2006.
- [4] J. B. Knight, A. Vishwanath, J. P. Brody, and R. H. Austin, "Hydrodynamic focusing on a silicon chip: Mixing nanoliters in microseconds," *Phys. Rev. Lett.*, vol. 80, no. 17, pp. 3863–3866, Apr. 1998.
- [5] J. Gao, X.-F. Yin, and Z.-L. Fang, "Integration of single cell injection, cell lysis, separation and detection of intracellular constituents on a microfluidic chip," *Lab Chip*, vol. 4, no. 1, pp. 47–52, Feb. 2004.
- [6] M. A. Unger, H.-P. Chou, T. Thorsen, A. Scherer, and S. R. Quake, "Monolithic microfabricated valves and pumps by multilayer soft lithography," *Science*, vol. 288, no. 5463, pp. 113–116, Apr. 2000.
- [7] F. Lin and E. C. Butcher, "T cell chemotaxis in a simple microfluidic device," *Lab Chip*, vol. 6, no. 11, pp. 1462–1469, Nov. 2006.
- [8] P. J. A. Kenis, R. F. Ismagilov, and G. M. Whitesides, "Microfabrication inside capillaries using multiphase laminar flow patterning," *Science*, vol. 285, no. 5424, pp. 83–85, Jul. 1999.
- [9] T. Pfohl, F. Mugele, R. Seemann, and S. Herminghaus, "Trends in microfluidics with complex fluids," *ChemPhysChem*, vol. 4, no. 12, pp. 1291–1298, 2003.
- [10] M. Z. Bazant and Y. Ben, "Theoretical prediction of fast 3D AC electro-osmotic pumps," *Lab Chip*, vol. 6, no. 11, pp. 1455–1461, Nov. 2006.
- [11] T. M. Squires and M. Z. Bazant, "Induced-charge electro-osmosis," *J. Fluid Mech.*, vol. 509, pp. 217–252, 2004.
- [12] C. L. Hansen, E. Skordalakes, J. M. Berger, and S. R. Quake, "A robust and scalable microfluidic metering method that allows protein crystal growth by free interface diffusion," *Proc. Nat. Acad. Sci. U.S.A.*, vol. 99, no. 26, pp. 16531–16536, Dec. 2002.
- [13] O. D. Velev and K. H. Bhatt, "On-chip micromanipulation and assembly of colloidal particles by electric fields," *Soft Matter*, vol. 2, no. 9, pp. 738–750, 2006.
- [14] R. Seemann, E. J. Kramer, and F. F. Lange, "Patterning of polymers: Precise channel stamping by optimizing wetting properties," *New J. Phys.*, vol. 6, p. 111, 2004.
- [15] H. Gau, S. Herminghaus, P. Lenz, and R. Lipowsky, "Liquid morphologies on structured surfaces: From microchannels to microchips," *Science*, vol. 283, no. 5398, pp. 46–49, Jan. 1999.
- [16] B.-J. de Gans and U. S. Schubert, "Inkjet printing of polymer microarrays and libraries: Instrumentation, requirements, and perspectives," *Macromolecul. Rapid Commun.*, vol. 24, no. 11, pp. 659–666, 2003.
- [17] E. Delamarche, D. Juncker, and H. Schmid, "Microfluidics for processing surfaces and miniaturizing biological assays," *Adv. Mater.*, vol. 17, no. 24, pp. 2911–2933, 2005.
- [18] N. E. Chayen, "The role of oil in macromolecular crystallization," *Structure*, vol. 5, no. 10, pp. 1269–1274, 1997.
- [19] B. Zheng, L. S. Roach, and R. F. Ismagilov, "Screening of protein crystallization conditions on a microfluidic chip using nanoliter-size droplets," *J. Amer. Chem. Soc.*, vol. 125, no. 37, pp. 11170–11171, 2003.
- [20] V. Rastogi and O. D. Velev, "Development and evaluation of realistic microbioassays in freely suspended droplets on a chip," *Biomicrofluidics*, vol. 1, pp. 014107-1–014107-17, 2007.
- [21] H. Yu, J. W. Kwon, and E. S. Kim, "Chembio extraction on a chip by nanoliter droplet ejection," *Lab Chip*, vol. 5, no. 3, pp. 344–349, Mar. 2005.
- [22] C.-Y. Lee, H. Yu, and E. S. Kim, "Microreactions using nanoliter droplets with oil encapsulation," in *Proc. IEEE Int. Micro Electro Mech. Syst. Conf.*, Kobe, Japan, Jan. 21–25, 2007, pp. 81–84.
- [23] C.-Y. Lee, H. Yu, and E. S. Kim, "Acoustic ejector with novel lens employing air-reflectors," in *Proc. IEEE Int. Micro Electro Mech. Syst. Conf.*, Istanbul, Turkey, Jan. 22–26, 2006, pp. 170–173.
- [24] S. A. Elrod, B. Hadimioglu, B. T. Khuri-Yakub, E. G. Rawson, E. Richley, C. F. Quate, N. N. Mansour, and T. S. Lundgren, "Nozzleless droplet formation with focused acoustic beams," *J. Appl. Phys.*, vol. 65, no. 9, pp. 3441–3447, May 1989.
- [25] R. Papen, R. Ellson, and J. Olechno, "Sound effects," *Amer. Lab.*, vol. 36, no. 24, pp. 26–31, Dec. 2004.
- [26] H. Zhang and W. Davison, "Performance characteristics of diffusion gradients in thin films for the in situ measurement of trace metals in aqueous solution," *Anal. Chem.*, vol. 67, no. 19, pp. 3391–3400, 1995.
- [27] J. M. Lopez-Cepero, "Silver carbonate staining reveals mitochondrial heterogeneity," *J. Histochem. Cytochem.*, vol. 52, no. 2, pp. 211–216, 2004.
- [28] C. H. Sorum, F. S. Charlton, J. A. Neptune, and J. O. Edwards, "pH change as an index to reaction mechanisms," *J. Amer. Chem. Soc.*, vol. 74, no. 1, pp. 219–221, 1952.



Chuang-Yuan Lee received the B.S. and M.S. degrees in electrical engineering from the National Taiwan University, Taipei, Taiwan, in 1999 and 2001, respectively, and the Ph.D. degree in electrical engineering from the University of Southern California (USC), Los Angeles, in 2007.

He is currently a Postdoctoral Research Associate with the Department of Electrical Engineering—Electrophysics, USC. His research interests include microelectromechanical systems, acoustic and piezoelectric transducers, microfluidic systems, and metal–oxide–semiconductor devices.



Hongyu Yu (M'03) received the B.S. and M.S. degrees in electronics engineering from the Tsinghua University, Beijing, China, in 1997 and 2000, respectively, and the Ph.D. degree in electrical engineering from the University of Southern California (USC), Los Angeles, in 2005.

He is currently a Postdoctoral Research Associate with the Department of Electrical Engineering and the Department of Biomedical Engineering and Cardiovascular Medicine, USC. His research focuses on various MEMS areas, such as RF-MEMS, bio-MEMS, and MEMS sensing. He has also worked on RF circuit design based on MEMS components and micrototal analysis system integration with acoustic transducers.



Wei Pang (S'04–M'06) was born in Chongqing, China, on February 11, 1980. He received the B.S. degree in precision instruments engineering from the Tsinghua University, Beijing, China, in 2001, and the M.S. and the Ph.D. degrees in electrical engineering from the University of Southern California, Los Angeles in 2006.

Since February 2006, he has been with the Wireless Semiconductor Division, Avago Technologies, Inc., San Jose, CA. Since 2004, he has published 28 articles in peer-reviewed leading journals and conferences in the area of MEMS for RF wireless communications, biological detection, wireless sensor platforms, and medical ultrasounds. His general research interests are in the areas of micro/nanofabrication, packaging, and merged CMOS-MEMS/NEMS technologies.



Eun Sok Kim (M'91–SM'01) received the B.S. (with high honors), M.S., and Ph.D. degrees in electrical engineering from the University of California, Berkeley, in 1982, 1987, and 1990, respectively. His doctoral dissertation was on the integrated microphone with large-scale integrated CMOS on a single chip.

Previously, he was with the IBM Research Laboratory, San Jose, CA, NCR Corporation, San Diego, CA, and Xicor Inc., Milpitas, CA, as a co-op student, Design Engineer, and summer student engineer, respectively. From the spring of 1991 to the fall of 1999, he was with the Department of Electrical Engineering, University of Hawaii, Manoa, Honolulu, as a faculty member. Since the fall of 1999, he has been with the University of Southern California, Los Angeles, where he is currently a Professor with the Department of Electrical Engineering. His research interests include micro-electromechanical systems, acoustic and piezoelectric transducers, microfluidic systems, microfabrication processing technology, and material study.

Dr. Kim serves on the editorial board for *Journal of Micromechanics and Microengineering*. He has been awarded a Research Initiation Award (FY 91–93) and a Faculty Early Career Development (CAREER) Award (FY 95–99) by the National Science Foundation. He received the Outstanding EE Faculty of the Year Award (voted by UH IEEE student chapter) in May 1996 and the IEEE TRANSACTIONS ON AUTOMATION SCIENCE AND ENGINEERING 2006 Best New Application Paper Award.